Reaction Sites in Thermo- and Photo-induced CO Oxidation on Stepped Pt(113) and the Collimation of Product Desorption(CO oxidation on Pt(113))

Sci. Rep. RITU A44 (1997) pp. 215-221
No. 2, March 1997

Reaction Sites in Thermo- and Photo-induced CO Oxidation on Stepped Pt(113) and the Collimation of Product Desorption

Tatsuo Matsushima, Toshiro Yamanaka, and Yuichi Ohno

Catalysis Research Center, Hokkaido University, Sapporo 060, Japan

(Received January 21, 1997)

The reaction sites in the thermal and photolytic CO oxidation on Pt(s)2(111)x(001) were examined through analysis of the angular and velocity distributions of desorbing product CO_2. In the former, the CO_2 desorption is sharply collimated but fairly shifted from the site normal, although the reaction proceeds on hollow sites of (100) and (111) patches. On the other hand, CO_2 produced in the photo-reaction is desorbed sharply along the (100) and (111) plane normal. This difference in the collimation is explained by reducing surface smoothing effect due to high velocity of desorbing CO_2.

KEYWORDS: reaction site, angular distribution, stepped surfaces, thermal desorption, photo-induced reaction

1. Introduction

Reaction site identification is requisite for designing catalyst surfaces with new functions as well as for developing surface molecular dynamics. Angular distributions of desorbing products provide direct structural information on reaction sites when the molecules are repulsively desorbed.[1] The orientation of reaction sites is determined from the collimation angle of desorbing products. The reaction sites analyzed in this way for the CO oxidation on platinum surfaces are always on hollow sites suitable for oxygen adsorption. This is consistent with high surface mobility of CO over oxygen adatoms.[2,3] However, there is always a significant difference between the collimation angle and the site normal, which sometimes yields ambiguity in assigning reaction sites. It was explained to be due to surface distortions and the surface smoothing effect by conduction electrons, since the product CO_2 interacts repulsively with the electronic surface rather than the plane defined by the localized atomic cores.[1]

The collimation angle of desorbing species has been believed to be very close to the ruptured bond angle in ESDIAD (electron stimulated desorption ion angular distribution) when the desorption is collimated not far from the surface normal.[4,5] In both ESDIAD and product CO_2 desorption, the desorption event should be repulsive with surfaces, i.e., with the adsorption site in ESDIAD or with the reaction site in the other. It is unrealistic to assume that the rotation or vibration of leaving species changes the collimation angle only in the thermal reaction, since the interval required to pass the surface interaction zone of a few Ångstrom is estimated to be in the order of 10^{-13} second in both cases. This is too short to interact with the surface changing the collimation. Probably, only a small fraction of the leaving molecules will receive such torque like as the rainbow scattering.[6] Rather a high translational energy in ESDIAD may reduce the surface smoothing effect, since the higher the velocity is, the more deeply the species interacts with the surface. In fact, the translational temperature of desorbing species in ESDIAD is one order higher than that of thermal reaction products at most. This consideration leads to the idea that the desorbing product with higher velocity may be collimated close to the site normal. In this paper, we have compared the collimation angle and velocity of desorbing product CO_2 in the thermal reaction with those in the photo-induced process. The collimation angle is confirmed to be close to the site normal in the photo-reaction where the velocity of products is enhanced.

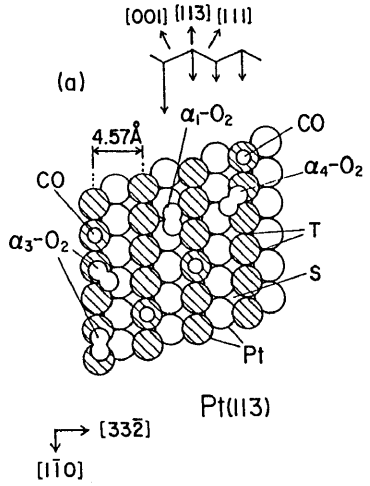

Fig. 1: Surface structure of Pt(113) and adsorbate distribution. The cross-hatched circles indicate protruding platinum atoms. The ellipses and the small circles show oxygen and CO molecules, respectively. Threefold and fourfold hollow sites are shown by T and S.

A stepped surface Pt(113)=(s)2(111)x(001) is suitable for this kind of experiments. It has two-atom wide (111) terraces with three-fold hollow sites and one-atom high (001) steps with four-fold hollow sites as shown in Fig. 1. These hollow sites are suitable for oxygen adsorption and decline alternately by +29.5° (terrace site) and -25.2° (step site) from the bulk surface plane. The product desorption from each site can be monitored separately by angle-resolved mass spectrometry.[1]

2. Experimental

The apparatus used for the thermal reaction consisted of a reaction, a chopper and an analyzer chamber,

pumped separately as shown in Fig. 2. The reaction chamber had LEED-AES optics, an Ar^+ gun and a mass spectrometer. The chopper chamber had a slit on each end, and a pseudo-random chopper blade for velocity measurements. A gate time of 15 μs is obtained at a chopper rotation of 130 Hz. CO_2 molecules produced on the sample surface (10 mm diameter 1 mm thick) were detected, after passing the two slits, by the other mass spectrometer in the analyzer chamber. The crystal was set on thin tantalum wires connected to gold rods cooled by liquid nitrogen and rotated to change the desorption angle θ (polar angle). The surface was cleaned by repeated cycles of Ar^+ bombardment and heating in 5×10^{-8} Torr oxygen at 850 K. Finally, it was annealed to 1200 K, and then showed LEED patterns characteristic of the stepped structure.[7]

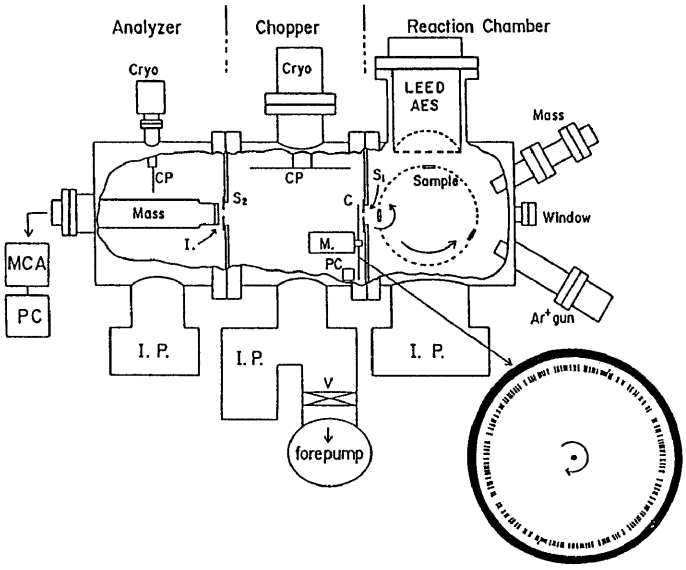

Fig. 2: Apparatus for angle-resolved thermal desorption incorporating a cross-correlation time of flight technique. S1, S2; slit, I; ionizer, C; random chopper (shape detailed in insert), M; motor, PC; photo-cell for trigger, CP; cryogenic plate, IP; ion pump, TP; turbo-molecular pump, V; isolation valve.

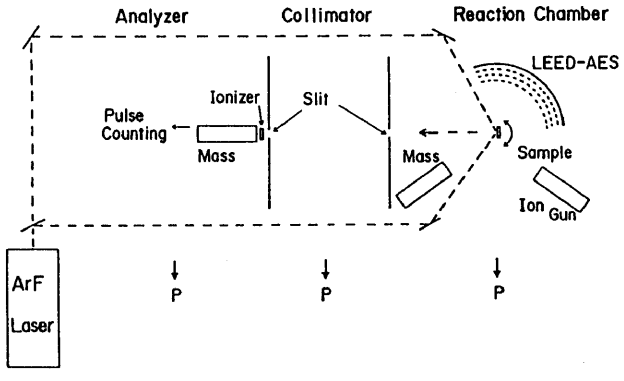

Fig. 3: Apparatus for photo-induced reaction measurements. Laser irradiation is introduced to the sample surface in two ways, so that the desorption angle can be varied in a wide range.

$^{18}O_2$ and $^{12}C^{16}O$ were sequentially dosed to the clean surface, and heated at a constant rate, or a non-polarized ArF (193nm) laser beam with a fluence of 1 mJ/cm^2 was incident at 5 Hz on the crystal for 6 minutes (Fig. 3). The product $^{12}C^{16}O^{18}O$ was detected with the mass spectrometer in the analyzer. The number of photons onto the surface was kept constant while the incident angle of the irradiation was varied.

The coverages of CO, O_2 and O, Θ_{CO}, Θ_{O_2} and Θ_O, were determined by TDS (thermal desorption spectroscopy). First, the coverage ratio of CO to oxygen was determined from desorption peak areas of CO, O_2 and CO_2, and the mass spectrometer sensitivity. The absolute coverage of CO was estimated by assuming that CO adsorbs on each step Pt atom at saturation.[8] The absolute coverage of CO and oxygen molecules at saturation is 0.85 ML and 0.67 ML, respectively.

3. Results

A. Thermal CO_2 formation

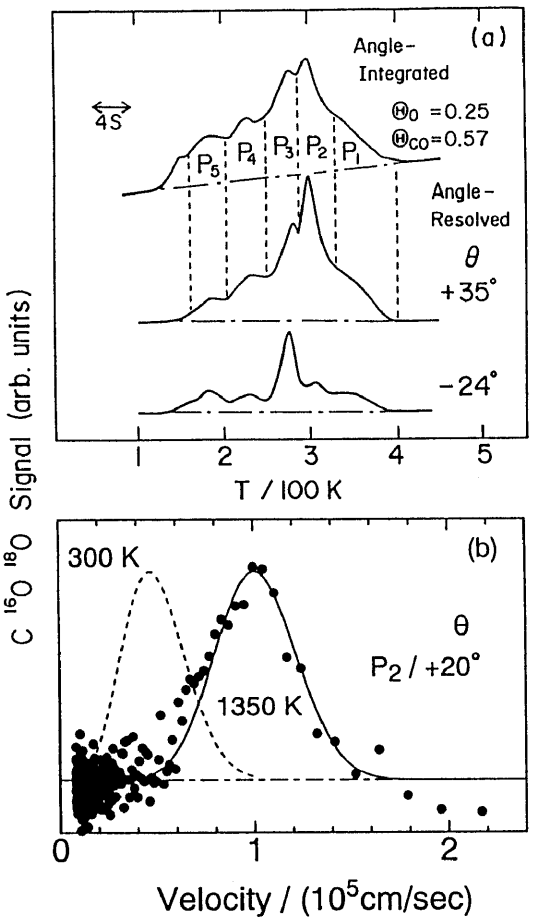

Fig. 4: (a) CO_2 formation spectra in angle-integrated and angle-resolved form at Θ_O =0.25 and Θ_{CO} =0.57. (b) Velocity distribution of desorbing P_2-CO_2 at θ = +20° in the direction up the step. The solid curve was obtained by the curve fitting to a modified Maxwellian form. The $T_{<E>}$ value is inserted. A Maxwellian distribution at the surface temperature is drawn by the broken curve.

Typical CO_2 formation spectra are shown in both angle-integrated and -resolved form in Fig. 4a. Oxygen was adsorbed dissociatively at 240 K and then CO was dosed below 150 K. A single peak of P_1-CO_2 is observed around 370 K at small coverages. With increasing coverages, the CO_2 formation extends to lower temperatures. Five CO_2 peaks are observed, at 370 K (P_1-CO_2), 300 K (P_2-CO_2), 270 K (P_3-CO_2), 235 K (P_4-CO_2), and 180 K (P_5-CO_2), at high initial coverages. These peak positions were determined by curve fitting with five Gaussians.

B. Angular distribution

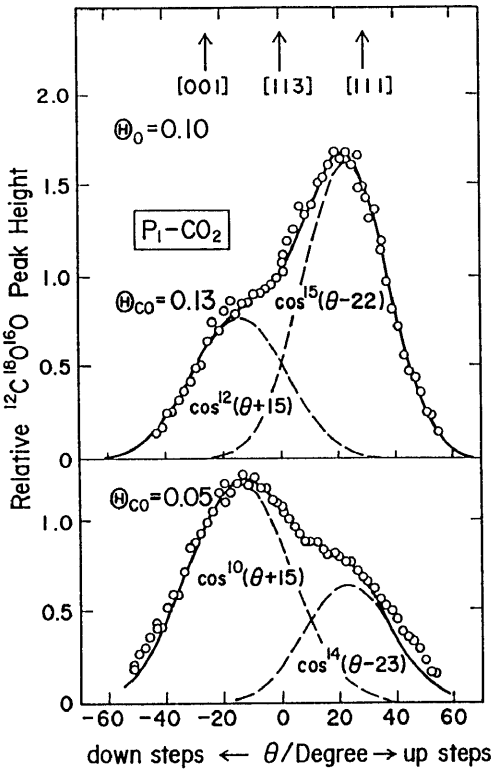

Fig. 5: Angular distribution of P_1-CO_2 at different CO coverages in the direction of up-and-down steps. The normal direction of (001), (113) and (111) plane is shown by the arrows.

The angular distribution depends strongly on the crystal azimuth. The distribution along the step edges in the [1$\bar{1}$0] direction is simply and sharply collimated toward the surface normal and is approximated by a $\cos^{7\sim10}(\theta)$ form. The distribution is more interesting in the direction of up-and-down steps as shown in Figs. 5 and 6. The distribution of P_1-CO_2 involves two components with simple cosine power functions of the desorption angle. The components are sharply collimated at θ = +23±2° close to the terrace normal and θ = -15±2° close to the step normal. The former is due to the reaction on the terraces and the latter on the steps. The latter becomes predominant at small Θ_{CO}, whereas the former becomes a major component at high CO coverage. The contribution from each component changes drastically by a small increment of CO coverage around Θ_{CO} = 0.07. Figure 6b shows the angular distributions of P_2-CO_2 , P_3-CO_2 and P_4-CO_2, which appear at high CO coverage. These distributions are commonly collimated at θ = +21±2°. These CO_2 are produced on the terraces. Only P_3-CO_2 shows a significant contribution from the step site.

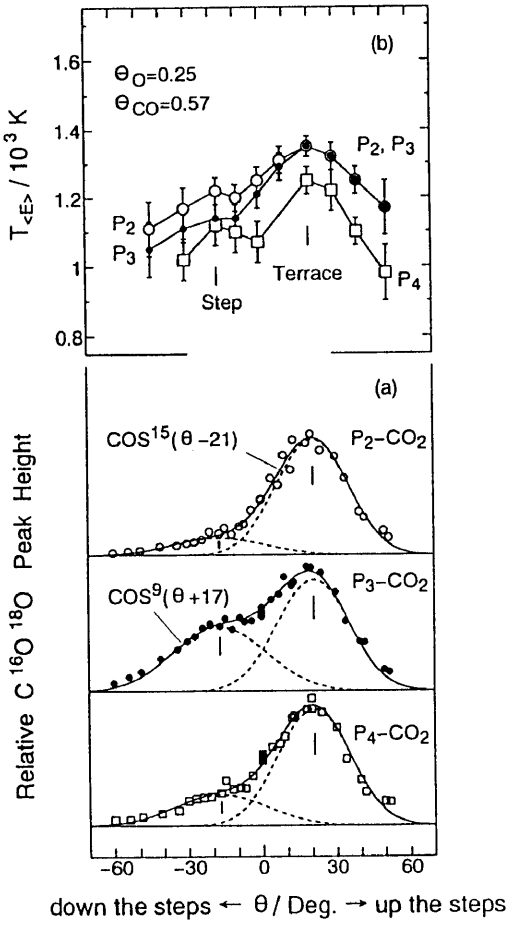

Fig. 6: (a) Angular distribution of P_2-, P_3-, P_4-CO_2 in the direction up and down the steps, and (b) desorption angle dependence of their translational temperatures. TDS was started at Θ_{CO} =0.25 and Θ_{CO} =0.57.

C. Translational temperature

A typical velocity distribution is shown in Fig. 4b. It shifts largely from a Maxwellian form at the surface temperature of 300 K drawn by the broken curve. The mean translational energy, <E>, was obtained by means of curve fitting to a modified Maxwellian form and represented in the temperature unit as $T_{<E>}$ = <E>/2k, where k is the Boltzmann constant. The $T_{<E>}$ values for P_2-, P_3-, and P_4-CO_2 are plotted as a function of θ in Fig. 6b. They show maximum values at the collimation angle. The value of 1350±30K was obtained for P_2- and P_3-CO_2 ,and 1250±40K for P_4-CO_2. These are about 4~5 times higher than the surface temperature. A strong repulsive force is operative to desorbing CO_2. The $T_{<E>}$ value decreases with increasing shift from the collimation angle and shows a small hump around θ =-17° where CO_2 is mostly desorbed from the steps. Thus, the decrement of 210 K is found in the translational temperature for P_3-CO_2 from the steps as compared with that from the terrace. A less decrement is found for P_2- and P_4-CO_2.

D. Photo-reaction product

The desorption of photo-reaction product CO_2 is found only in the presence of oxygen admolecules.[9] Its

angular distribution is sensitive to the O_2 and CO coverages. The desorption of CO_2 in a plane along the troughs at three O_2 coverages is shown in Fig. 7. It was measured only in a positive angle range because of the surface symmetry. The CO_2 desorption at low oxygen and CO coverages is collimated sharply at $\theta = +23°$, indicating two-directional form peaking at ±23°. In fact, the distribution data can be fitted by a function of $\cos^{15}(\theta+23)+\cos^{15}(\theta-23)$ as drawn by the solid line. The distribution at $\Theta_{O_2} = 0.25$ is split into two components peaking ±20°. The distribution at $\Theta_{O_2} = 0.67$ may be deconvoluted into two components peaked at $\theta = \pm 13°$. A similar coverage effect of CO was found on the distribution along the trough as shown in Figs. 8a and b.

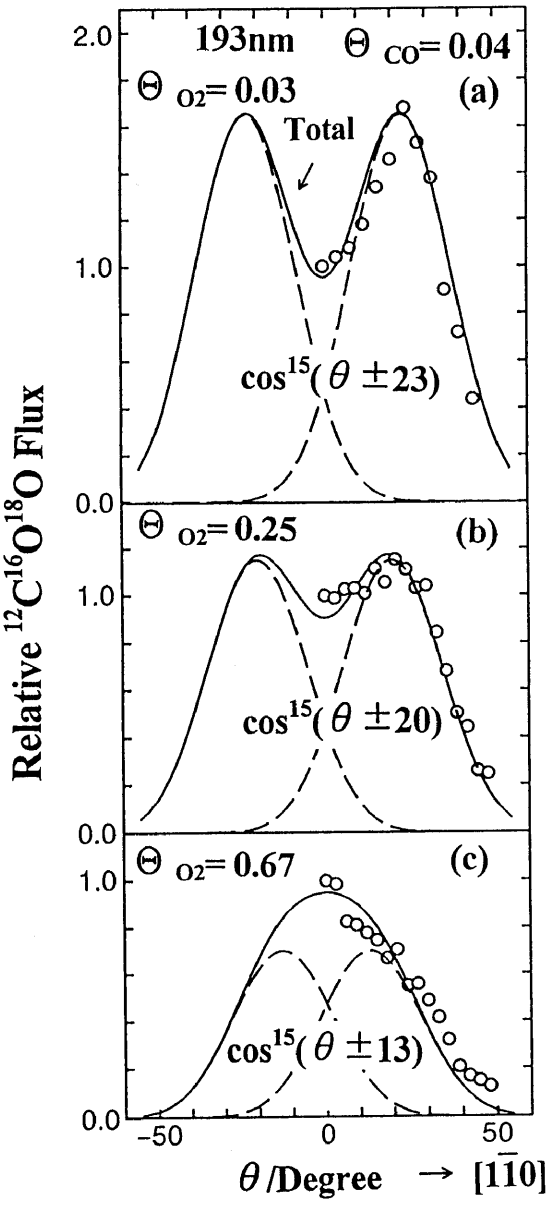

Fig. 7: Angular distributions of desorbing photo-reaction product CO_2 in a plane along the surface trough at various O_2 coverages.

The distribution is more interesting in the direction of up-and-down steps as shown in Fig. 9. At low coverages, it shows a single peak of $\cos^{14}(\theta-2)$ collimated closely along the bulk surface normal, confirming the two-directional desorption oblique along the trough. At high O_2 coverage, two additional desorption components grow, being collimated at $\theta = +28°$ and -24°. The former is collimated along the (111) terrace normal at 29.5°. The latter increases rapidly above $\Theta_{O_2} = 0.25$ and is collimated closely along the (001) step normal at -25.2°. The remaining component after the subtraction of the above components of $\cos^{30}(\theta-28)$ and $\cos^{14}(\theta+24)$ is collimated closely to the normal direction. It becomes sharper with increasing O_2 coverage. On the other hand, the distribution at $\Theta_{CO} >> \Theta_{O_2}$ is collimated closely along the surface normal, i.e., the distribution is in the form of $\cos^{15}(\theta-5)$ up-and-down the steps and also simply collimated along the normal perpendicular to it (Fig. 8). The components along the (111) and the (001) normal are mostly suppressed.

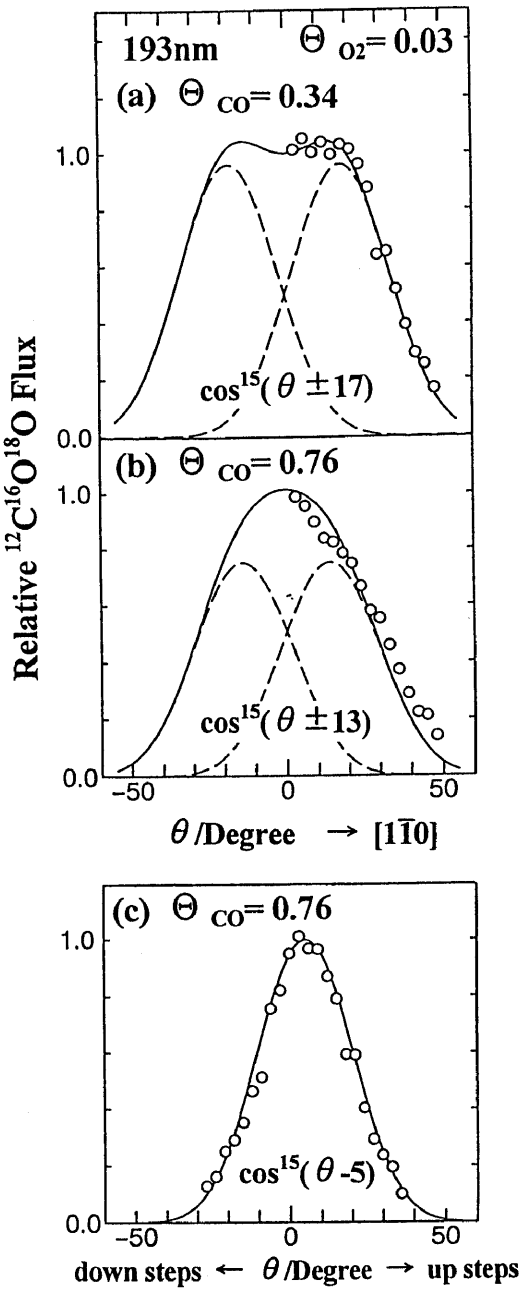

Fig. 8: Angular distribution of CO_2 in the photo-reaction at different CO coverages.

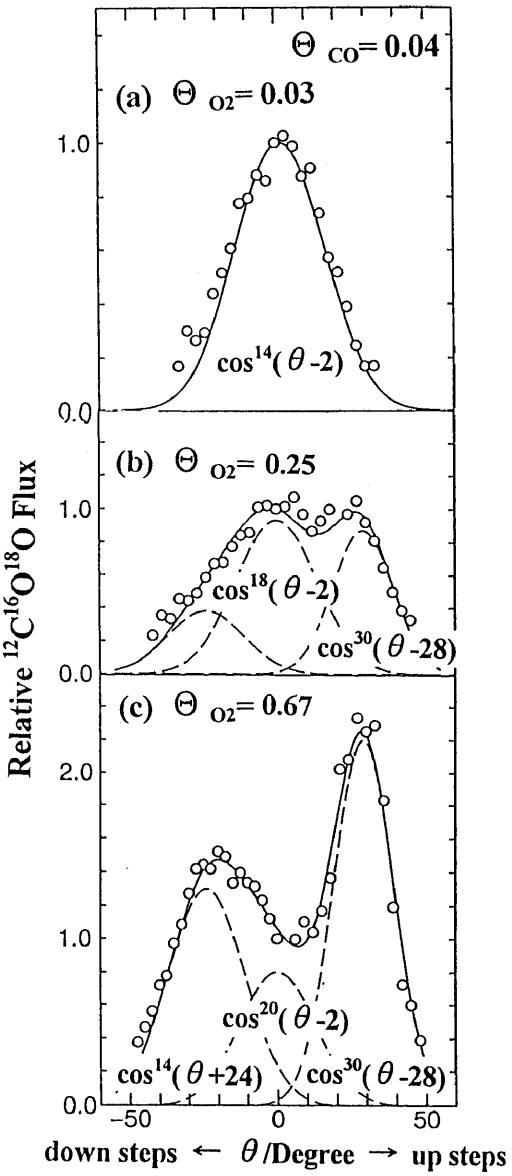

Fig. 9: Angular distributions of CO_2 in the photo-reaction at different O_2 coverages in the direction of up and down the steps.

E. Translational energy

In the repulsive desorption, the angle dependence of the translational energy provides the orientation of reaction sites. Typical velocity distribution curves at various angles are shown in Fig. 10, where the angle is shifted in a plane along the trough. These curves are deconvoluted into three components by assuming a modified Maxwellian form to each. The velocity curves at Θ_{O_2} =0.03 and Θ_{CO}= 0.04 consist of three components with energies below 340 K, and of 1100-1500 K and 2900-3500 K. The first component contributes negligibly to the total energy. The second is collimated along the surface normal and becomes predominant at high O_2 coverages. The third should be noticed to peak around θ =36° and disappears at high O_2 coverage, where a very fast component of 7200 K is newly observed at the surface normal (Fig. 10e). On the other hand, at high CO coverage, only a single component is found in the velocity curves and the translational energy is fairly constant around 2000 K. At high O_2 coverage, the mean translational energy increases sharply around the bulk surface normal. This energy around the normal direction is rather decreased with decreasing Θ_{O_2}. Eventually, the energy is maximized around θ =30~35° at lower O_2 coverage.[10]

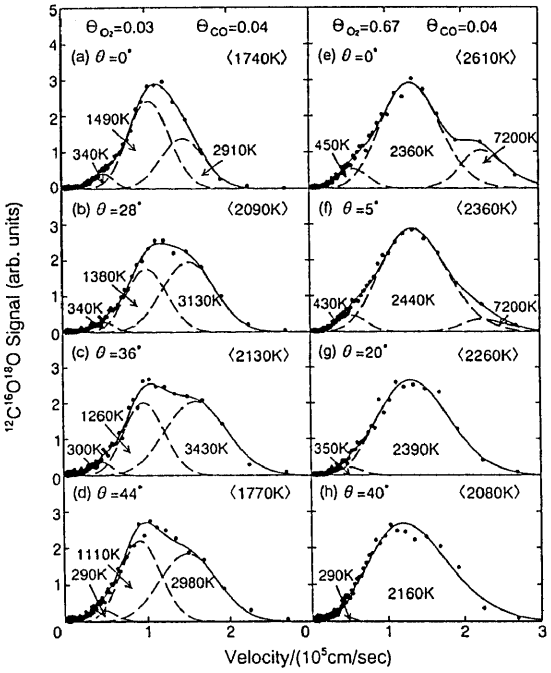

Fig. 10: Velocity distribution curves of desorbing photo-reaction product CO_2 at various desorption angles in a plane along the trough. (a-d) Θ_{O_2}= 0.03 and (e-f) Θ_{O_2} = 0.67. The mean translational temperature is in the parentheses. The temperature of each component is also shown.

The angle-dependence of the mean energy in the direction of up-and-down steps is shown in Fig. 11. The results support the presence of the desorption components along the (001) and (111) plane normal. The energy shows two maxima around θ = -24° and θ =+28° at Θ_{O_2}=0.25, being consistent with the results in Fig. 9. Furthermore, an additional maximum appears around θ = 0° in the angle-dependence at Θ_{O_2}=0.67. This is caused by the appearance of the component of 7200 K.

4. Discussion

A. Site switching

The thermal oxidation of CO on platinum metals takes place on oxygen adsorption sites.[1] On the present surface, there are one kind of fourfold hollow sites on the (001) steps and two kinds of threefold hollow sites on the (111) terraces. These sites are suitable for oxygen adsorption and then for CO oxidation. In fact, the product CO_2 desorption is sharply collimated closely to the normal direction of the step and terrace. Furthermore, the reaction site is switched from the step to terrace sites with increasing CO coverage. Such switching was expected from the ESDIAD results,[8] where oxygen located on the steps of Pt(112) was observed to be repelled to the terraces by post-dosed CO. The present experiments indicate that the site switching is completed at fairly small CO coverages. The reaction occurs mostly on the terrace.

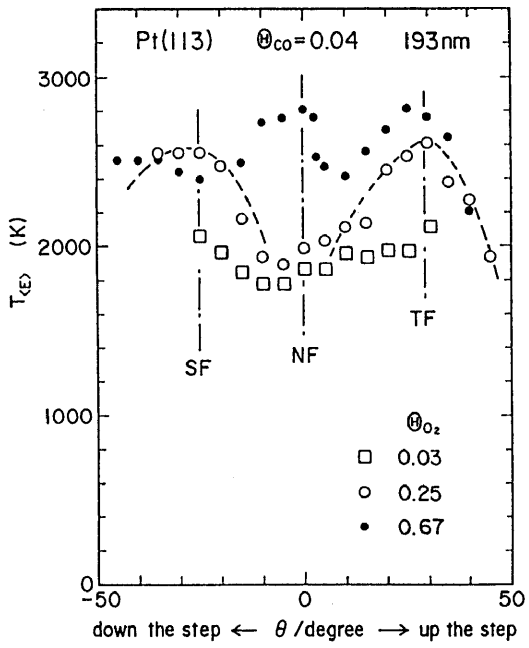

Fig. 11: Variation of the translational temperature with the desorption angle at different O_2 coverages. The vertical lines indicate the angles at the (111) terrace normal (TF), the (001) step normal (SF) and the bulk surface normal (NF).

The reaction site in the photo-induced process is mostly determined by the distribution of oxygen admolecules. These molecules lie along the surface trough in a wide coverage range.[11] At small coverage, the molecules are located mostly in the trough as sketched as α_1-O_2 in Fig. 1, whereas they are also populated on the terrace and then the steps with increasing coverage as shown by α_3-O_2 and α_4-O_2.

At small coverages, hot oxygen atoms are emitted along the trough and react with CO on the top of protruding platinum atoms. The product CO_2 will receive a repulsive force along the surface normal at the moment of the formation.[1] Thus, the fast CO_2 desorption is collimated far from the bulk surface normal in a plane along the trough and shows the maximum energy (~3500K) around θ=36°. The momentum of the hot oxygen atom is partly retained in this associative desorption event. The life time of the activated complex $(CO+O)^*$ is short. The component of 1100-1500 K is formed from a similar reaction, but with the activated state of a longer life time, or from the reaction of CO with excited O_2 molecules.[9,12]

The desorption components collimated along the (111) terrace and the (001) step, and the bulk surface normal grow at higher O_2 coverage. These have no sign of retaining the parallel hot atom momentum, since the desorption component along the trough is suppressed, although oxygen admolecules are mostly oriented along the trough even at high O_2 coverage. Only a small fraction of them is oriented in different ways as shown by α_4-O_2. Here, the other interaction must be invoked for these components. At high CO coverage, CO occupies every step platinum atom and O_2 is located only in the trough because of a high heat of adsorption of CO. This explains that both (111) terrace and (001) step components are suppressed. At high O_2 coverages, the distance of O_2 to CO becomes short (Fig. 1) and the reaction occurs when O_2(a) is excited by the irradiation. The resultant product desorption is directed along the (111) terrace or the (001) step normal. Excited O_2 in the trough may react with CO, yielding the high velocity component.

B. Collimation angle

The collimation angle in the thermal reaction is largely shifted from the site normal. The collimation angles reported so far are summarized in Fig. 12.[1] The solid line named by "ideal" shows the relation between the collimation and site declining angle, where no distortion is assumed in the surface layer and the product is desorbed along the site normal. The experimental values are about 30 % smaller than this line. Two factors have been proposed for this discrepancy; the stepped surfaces are likely to be largely distorted, i.e., protruding atoms are moved towards the bulk crystal so that both the step and terrace may decline less than the above ideal case. The extent of such distortion was analyzed on clean Pt(110)(1x2).[13] The broken line in the figure is drawn according to this analysis where the declining angle is reduced about 15%. However, this is overestimated, since the surface covered by chemisorbed species is less distorted than the clean surface.[14] The collimation angle is expected to be in the cross-hatched region in Fig. 12. The observed angles are still less than this level. This difference has been explained by the second factor, i.e., the surface smoothing effect by conduction electrons. It may be reduced by increasing velocity of desorbing products.

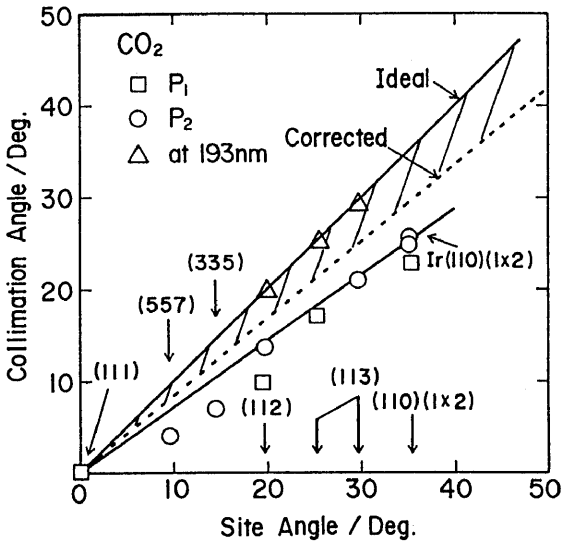

Fig. 12: Plot of the CO_2 desorption collimation angle versus the declining angle of terraces on various stepped surfaces. The declining angle of the step is referred to as P_1-CO_2 on Pt(113). The solid line shows the relation which would be observed when the CO_2 desorption is collimated along the normal of the non-distorted terrace. The dashed line indicates the relation after correcting the surface distortions.

The triangles in Fig. 12 indicate the collimation angles in the photo-reaction. The photolytic CO_2 desorption on Pt(112) is quite similar to that on Pt(113).[15] It is

sharply collimated along the (111) terrace normal at high O_2 coverages. These collimation angles are very close to the site normal. No smoothing effect is invoked. About two times difference is found in the translational energy of desorbing products between the thermal and photo-reaction. This indicates that the collimation angle becomes insensitive to the transaltional energy when the energy is just above that of the thermal reaction product.

Acknowledgement

This work was supported in part by Grant-in-Aid No. 06403012 for Scientific Research (a) from the Ministry of Education of Japan.

1) T. Matsushima, Heterogeneous Chemistry Review, **2** (1995) 51.
2) J. E. Reutt-Robey, D. J. Doren, Y. J. Chabal and S. B. Christman, Phys. Rev. Lett. **61** (1988) 2778.
3) H.H. Rotermund, Surf. Sci. **283** (1993) 87; A. Von Oertzen, H.H. Rotermund and S. Nettersheim, Surf. Sci. **331** (1994) 322 .
4) T.E. Madey, D.E. Ramaker and R. Stockbauer, Ann. Rev. Phys. Chem. **35** (1984) 215.
5) R.D. Ramsier and J.T. Yates, Jr., Surf. Sci. Rep. **12** (1991) 243 .
6) C.R. Arumainayagam and R.J. Madix, Prog. Surf. Sci., **38** (1991) 1.
7) T. Yamanaka, C. Moise and T. Matsushima, submitted to J. Chem. Phys. (1997).
8) A. Szabo, M. A. Henderson and J. T. Yates Jr., J. Chem. Phys. **96** (1992) 6191.
9) W.D. Mieher and W. Ho, J. Chem. Phys. **91** (1989) 2755.
10) T. Yamanaka, Y. Inoue and T. Matsushima, Chem. Phys. Lett. **264** (1996) 180.
11) T. Yamanaka, T. Matsushima, S. Tanaka and M. Kamada, Surf. Sci. **349** (1996) 119.
12) V.A. Ukraintsev and I. Harrison, J. Chem. Phys. **96** (1992) 6307.
13) E.C. Sowa, M.A. Van Hove and D.L. Adams, Surf. Sci. **199** (1988) 174.
14) M.A. van Hove: The Nature of the Surface Chemical Bond, eds. T.N. Rhodin and G. Ertl (North-Holland, Amsterdam, 1979) p. 274.
15) H. Sugimura and T. Matsushima, unpublished data.